FEBS Letters

FEBS PRESS science publishing by scientists

FRET-based binding assay between a fluorescent cAMP analogue and a cyclic nucleotide-binding domain tagged with a CFP

Francisco Romero, Carmen Santana-Calvo, Yoloxochitl Sánchez-Guevara and Takuya Nishigaki

Departamento de Genética del Desarrollo y Fisiología Molecular, Instituto de Biotecnología, Universidad Nacional Autónoma de México (UNAM), Cuernavaca, Morelos, México

Correspondence
T. Nishigaki, Departamento de Genética del Desarrollo y Fisiología Molecular, Instituto de Biotecnología, Universidad Nacional Autónoma de México (UNAM), Cuernavaca, Morelos 62210, México
Fax: + 52-777-3172388
Tel: + 52-777-3291709
E-mail: takuya@ibt.unam.mx

(Received 21 February 2017, revised 29 June 2017, accepted 18 July 2017, available online 20 August 2017)

doi:10.1002/1873-3468.12760

Edited by Michael Bubb

The cyclic nucleotide-binding domain (CNBD) functions as a regulatory domain of many proteins involved in cyclic nucleotide signalling. We developed a straightforward and reliable binding assay based on intermolecular fluorescence resonance energy transfer (FRET) between an adenosine-3′, 5′-cyclic monophosphate analogue labelled with fluorescein and a recombinant CNBD of human EPAC1 tagged with a cyan fluorescence protein (CFP). The high FRET efficiency of this method (~ 80%) allowed us to perform several types of binding experiments with nanomolar range of sample using conventional equipment. In addition, the CFP tag on the CNBD enabled us to perform a specific binding experiment using an unpurified protein. Considering these advantages, this technique is useful to study poorly characterized CNBDs.

Keywords: binding experiment; EPAC; equilibrium binding; molecular interaction

The cyclic nucleotide-binding domain (CNBD) is an evolutionarily conserved molecular switch that alters its conformation in response to cyclic nucleotides (cNMPs). The CNBD regulates the activity of several types of proteins such as transcriptional factors in prokaryotes, and kinases, ion channels and guanine nucleotide exchange factors in eukaryotes [1]. Recently, a novel functional CNBD was also reported as a testis specific protein named CRIS although its exact function remains unknown [2].

The activity of a CNBD can be determined by measuring cNMP dependence of each protein activity such as kinase activity for PKA, but it is also possible to study the molecular interaction between a cNMP and the whole protein or the isolated CNBD. For instance, a radioactively labelled cNMP can be used to determine specific binding to a CNBD by mechanical separation (i.e. filtration and centrifugation) of free and bound ligands [3]. When isothermal titration calorimetry is applied, the molecular interactions can be determined even using nonlabelled cNMP [4–6].

On the other hand, it is known that some chemically modified cNMP analogues, particularly at carbon-8 of the purine ring, can work as functional analogues for CNBDs [7]. Therefore, fluorescently labelled cNMPs, such as 8-(2-[Fluoresceinyl]aminoethylthio) adenosine-3′, 5′-cyclic monophosphate (8-Fluo-cAMP) and 8-(2-[7-Nitro-4-benzofurazanyl]aminoethylthio) adenosine-3′, 5′-cyclic monophosphate (8-NBD-cAMP) have been employed as useful fluorescent analogues of cNMP. In fact, 8-Fluo-cAMP, a bright fluorescent analogue of cAMP, has been largely used to determine the molecular interactions by means of fluorescence anisotropy [8,9]. In contrast, 8-NBD-cAMP, a dim fluorescent analogue, has been used to study some CNBDs since its fluorescence intensity changes several times depending on the polarity of the environment, namely upon the binding to a CNBD [5,6,10,11]. These methods based on

Abbreviations
CNBD, cyclic nucleotide-binding domain; cNMP, cyclic nucleotide; FRET, fluorescence resonance energy transfer.

fluorescence spectroscopy are useful but do not satisfy both sensitivity and versatility at the same time.

Taking this situation into account, we developed a simple technique to study the molecular interaction based on fluorescence resonance energy transfer (FRET) using 8-Fluo-cAMP and a recombinant CNBD tagged with a cyan fluorescent protein (CFP). Our method is more sensitive and versatile than those reported previously.

Materials and methods

Materials

A plasmid encoding monomeric super enhanced CFP (mseCFP) in pRSETB (mseCFP-pRSETB) was provided by T. Nagai (Osaka University, Japan). There are several mseCFP isoforms developed in distinct laboratories, so we just called 'CFP' for mseCFP developed by T. Nagai in order to simplify the name in this work. A plasmid encoding the CNBD of human EPAC1 (EPAC1-camps, a genetically encoded fluorescent cAMP sensor) [12] was provided by M. Lohse (University of Wuerzburg, Germany). Fluorescent analogue of cAMP (8-Fluo-cAMP) was purchased from Axxora LLC (San Diego, CA, USA). Bacteria strains, JM109(DE3) and BL21(DE3) were obtained from the National BioResource Project *Escherichia coli* strain, National Institute of Genetics (Mishima, Shizuoka). Most of the enzymes for molecular biology were purchased from Fermentas Inc. (Glen Burnie, MD, USA) except for Vent® DNA Polymerase from New England Biolabs (Ipswich, MA, USA). cOmplete™, Protease Inhibitor Cocktail Tablet, was from Roche (Basel, Schweiz).

Preparation of plasmids

For $EPAC1_{CNBD}$-CFP construction, CNBD of human EPAC1 (E157-E316) was amplified by PCR using EPAC1-camps [12] as a template and the following oligonucleotides, forward (5′ GGC TAG CGA ATT CGA GGA GTT GGC C 3′) and reverse (5′ GGG ATC CCC TCT AGA TTC CAG CCG CA 3′). The amplified product was digested by *Nhe*I and *Bam*HI and inserted into mseCFP-pRSETB ($EPAC1_{CNBD}$-CFP-pRSETB).

Production of recombinant proteins

Bacteria strains, JM109 (DE3) or BL21 (DE3), were transformed with $EPAC1_{CNBD}$-CFP-pRSETB and the recombinant proteins were expressed by growing the cultures in 200 mL LB (shaking 200 r.p.m.) around 22 °C in the presence of ampicillin for 2 days without Isopropyl-β-D-thiogalactopyranoside [13]. Expression of the recombinant proteins can be confirmed by yellowish colour of the cell suspension. The bacterial cell pellets were spun down by centrifugation (2500 ***g*** for 20 min at 4 °C) and washed three times with solution A (150 mM NaCl and 10 mM Tris-HCl, pH 7.4). The washed bacterial pellets were suspended in 1 mL of solution A supplemented with protease inhibitors, cOmplete™. The bacteria were processed by brief sonication on ice (two to three times of 30 s of sonication with 90-s interval). The disrupted cells were centrifuged (28 000 ***g*** for 10 min at 4 °C) and the supernatant that contains the recombinant proteins was recovered as the unpurified recombinant protein and used for some experiments. For purification of the recombinant protein, this fraction was applied to 1 mL of Ni-NTA Superflow column (Qiagen, Hilden, Germany) equilibrated with solution A. Weakly bound endogenous bacterial proteins were washed out with 5 mL of solution A supplemented with 50 mM imidazole. The recombinant protein was eluted by addition of solution A supplemented with 250 mM imidazole (yellowish colour solution). The purified recombinant protein was confirmed as a major single protein stained by Coomassie Brilliant Blue in SDS/PAGE. The imidazole was removed by gel filtration with Sephadex-G25 (Pharmacia, Uppsala, Sweden) using solution A. The purified recombinant protein was concentrated using an Amicon Ultra 50 K filter (Cork, Ireland). We determined the concentration of the recombinant protein by measuring absorbance at 435 nm using NanoDrop™ 2000 (ThermoFisher Scientific, Waltham, MA, USA) in solution A (the molar extinction coefficient of CFP is 32 500 $M^{-1} \cdot cm^{-1}$). We also determined the concentration of the purified protein by Bradford assay using BSA as a protein standard, which was almost consistent with the value determined by absorbance of CFP (the difference was < 5%). In all binding experiments, solution A was used as a medium. In some experiments, we did not remove the imidazole from the purified protein and perform the binding assay in the presence of residual imidazole. We confirmed that 100 mM imidazole did not alter the dynamic K_d value between $EPAC1_{CNBD}$-CFP and 8-Fluo-cAMP as shown in Results section.

Spectrofluorometry

Fluorescence measurements were performed with Aminco SLM 8000 spectrofluorometer upgraded by Olis (Bogart, GA, USA) with a 450 W Xenon arc lamp as excitation light source. To obtain only emission spectra, we also used royal blue high power LED (Luxeon star V royal blue Lambertian; Lumileds Lighting LLC, San Jose, CA, USA) as an excitation light source instead of the Xenon arc lamp. Samples in the spectrofluorometer were illuminated through a liquid light guide attached to a LED holder where D440/20ex bandpass filter (Chroma Technology, Rockingham, VT, USA) was mounted. In general, fluorescence intensities and spectra of sample solutions (2 mL) were measured at room temperature using

disposable plastic cuvette (Polystyrene Fluorimeter cuvettes; Sigma-Aldrich, St. Louis, MO, USA). For concentrated samples (> 3 μM), 45 μL or 160 μL quartz cuvettes (16.45F-Q-3 or 16.160F-Q-10; Starna Cells, Inc., Atascadero, CA, USA) were used. Fluorescence determination was performed with, at least, triplicate samples.

Binding kinetics measurements by Stopped-Flow Spectrofluorometer

The k_{off} and k_{on} values between $EPAC1_{CNBD}$-CFP and 8-Fluo-cAMP were determined using a Stopped-flow Spectrofluorometer SFM-20 equipped with MOS-200 (BioLogic, Seyssinet-Pariset, France) at 22 °C. Each sample was excited by monochromatic light at 440 nm through an optical fibre and the fluorescence intensity was detected using long-pass filter (> 515 nm), which mainly corresponds to the acceptor fluorescence. The excitation light intensity was reduced by manipulating distance between the optical cell and the end of the optical fibre and/or altering the alignment of Xenon arc lamp to prevent photobleaching during the kinetics measurements. To elucidate the k_{off} value, $EPAC1_{CNBD}$-CFP and 8-Fluo-cAMP complex (each 100 nM) was mixed with an excess of competitor (10 μM 8-CPT-cAMP) at flow rate 2 mL·s^{-1}. To obtain the k_{on} value, 200 nM (100 nM at final) $EPAC1_{CNBD}$-CFP was mixed with 200 nM (100 nM at final) 8-Fluo-cAMP at flow rate 2 mL·s^{-1}. In both k_{off} and k_{on} measurements, fluorescence intensities were recorded every 10 ms for 80 and 15 s respectively. Three samples were prepared separately and the average of 16 traces was obtained from each sample.

With the acquired data, k_{on} and k_{off} values were calculated from the averaged fluorescence traces in each sample. The k_{off} value was obtained from the dissociation kinetics fitting to Eqn (1), where $F(t)$ is the fluorescence intensity of the acceptor (8-Fluo-cAMP) in function of time. Strictly speaking, the light detected through the long-pass filter (> 515 nm) includes the emission of fluorescein and a bleed-through of CFP. However, there is a linear relationship between the intensities of the detected light and the FRET efficiencies. The constants, α and β, allow fitting of the data (the fluorescence intensities) to the FRET efficiencies, which in turn represent the status of the molecular interactions (free or bound forms of ligand).

$$F(t) = \alpha\left(e^{-k_{off}t}\right) + \beta \tag{1}$$

After the k_{off} was determined, the k_{on} value was derived by fitting data to Eqn (2).

$$F(t) = \alpha'\left(\frac{a(1 - e^{(a-b)k_{on}t})}{1 - \frac{a}{b}e^{(a-b)k_{on}t}}\right) + \beta' \tag{2}$$

Wherein:

$$a, b = [R] + [L] + \frac{k_{off}}{k_{on}} \pm \frac{\sqrt{\left([L] + [R] + \frac{k_{off}}{k_{on}}\right)^2 - 4[R][L]}}{2}$$

Also, α′ and β′ are similar constants to α and β for the fitting of the association kinetics. Fitting was carried out using R [14].

Determination of dissociation constant (K_d) at equilibrium binding condition

To determine the K_d at equilibrium (static K_d), first we prepared 3.16 μM $EPAC1_{CNBD}$-CFP and 6.32 μM 8-Fluo-cAMP in the presence and absence of excess amount of competitor (1 mM 8-CPT-cAMP). Then, we performed serial dilution in disposable plastic cuvettes until $EPAC1_{CNBD}$-CFP reached 0.032 nM (using 3.16 as dilution factor). Fluorescence emission spectra excited by 440 nm light of all samples were measured using the Aminco SLM 8000 spectrofluorometer. Since fluorescence intensities were quite different depending on the concentration of the samples, we modified the voltage of the photomultiplier to obtain reasonable signals. In the diluted samples, we repeated the scan of spectra and obtained the average of traces (scan was carried out 20 times for the most diluted sample). We also measured basal signal of the medium, which is not negligible in the diluted samples, and obtained the net fluorescence signals by background subtraction. We added 0.1% BSA to all solution in this experiment to avoid a nonspecific binding.

Once the spectrum was corrected, we established the ratio between the fluorescence intensity of the FRET donor (at 474 nm) and that of the isosbestic point (at 501 nm; F_{474}/F_{501}). Our method is based on the theory of bimolecular (receptor–ligand) interaction with ligand depletion (Eqn (3)).

$$[RL] = \frac{[L]_T + [R]_T + K_d - \sqrt{([L]_T + [R]_T + K_d)^2 - 4[L]_T[R]_T}}{2} \tag{3}$$

Then, we simplified Eqn (3) considering the fact that $[L]_T = 2[R]_T$ ($[R]_T = x$, $[L]_T = 2x$) and the fraction of the ligand–receptor complex ($[RL]/[R]_T$) is proportional to relative FRET efficiency, which in turn has linear relationship with $-F_{474}/F_{501}$. Then, we obtained Eqn (4). Constants α″ and β″ are similar constants to constants α and β in Eqn (1).

$$\frac{-F_{474}}{F_{501}} = \alpha''\left(\frac{3x + K_d - \sqrt{(3x + K_d)^2 - 8x^2}}{2x}\right) + \beta'' \tag{4}$$

To determinate the value of K_d of each experiment, we established the best-fitting using Eqn (4) with R [14].

Competitive binding curves measured by fluorescence plate reader

Competitive binding assay was performed using four cNMP analogues (cAMP, cGMP, 8-CPT-cAMP and 8-CPT-cGMP) as competitors for 8-Fluo-cAMP binding to $EPAC1_{CNBD}$-CFP. Each competitor was diluted (dilution factor: 2) from 12.5 mM of 8-CPT-cGMP, 10 mM of cGMP, 1 mM of 8-CPT-cAMP and 100 μM of cAMP. The competitors were mixed with 10 nM of CNBD-CFP and 20 nM of 8-Fluo-cAMP in 96-well plates (Corning® 96 Well Flat Clear Bottom Black Polystyrene TC-Treated Microplates, Product #3603, Corning, NY, USA) and kept for 30 min at room temperature in the dark. The fluorescence intensities of the samples (200 μL) were measured with a fluorescence plate reader (FLUOstar omega microplate reader; BMG Labtech, Ortenberg, Germany) using 440 nm (10 nm) bandpass filter for excitation light and 485 nm (12 nm) bandpass filter for emission light. Fluorescence values were determined by background subtraction. Triplicated samples were prepared to obtain the average of each condition. We determined K_i values (K_d values between $EPAC1_{CNBD}$ and competitor) using the method of Wang [15].

Results

Fluorescence spectra

We chose 8-Fluo-cAMP as a fluorescent analogue of cAMP due to its high brightness and commercial availability (Fig. 1A upper right). Then, we used a cyan fluorescence protein (CFP) as a FRET donor for 8-Fluo-cAMP. Using the CNBD of human EPAC1, whose optimal expression condition in bacteria has been established [5,12], we prepared the CNBD tagged with CFP in the C terminus of CNBD ($EPAC1_{CNBD}$-CFP, Fig. 1A upper left) as described in Materials and methods. Lower parts of Fig. 1A shows fluorescence spectra of $EPAC1_{CNBD}$-CFP and 8-Fluo-cAMP. Fluorescence emission spectra of CFP and fluorescence excitation spectra of 8-Fluo-cAMP have a large spectral overlap (Fig. 1B), which favours high FRET efficiencies between two fluorophores. However, 8-Fluo-cAMP is slightly excited by the excitation light (440 nm) used in the assay (Figs 1C and 2B), which is an undesirable feature for a FRET pair and is discussed later.

Binding assay based on FRET

Figure 2A shows the fluorescence spectra of $EPAC1_{CNBD}$-CFP (donor) + 8-Fluo-cAMP (acceptor) in the presence or absence of an excess of nonfluorescent potent cAMP analogue, 8-CPT-cAMP, for binding competition [16]. As the spectrum clearly shows, the fluorescence intensity of CFP is smaller in the absence than that with the competitor (particularly the first emission peak), indicating that high level of FRET occurred between CFP and fluorescein in the absence of the competitor. That, in turn, indicates a specific binding between $EPAC1_{CNBD}$-CFP and 8-Fluo-cAMP. As mentioned previously, significant fluorescence is detected from the donor (fluorescein) alone (Fig. 2B green line). Therefore, the shape of fluorescence spectrum of $EPAC1_{CNBD}$-CFP + 8-Fluo-cAMP in the presence of the competitor (Fig. 2A black line) is distinct from that of $EPAC1_{CNBD}$-CFP alone (Fig. 2B blue line), rather it is nearly identical to the sum of fluorescence from individual fluorophores (Fig. 2B brown line). When only CFP (without the CNBD) was used in the assay, FRET was not observed at all (data not shown). Also, we produced a nonfunctional CNBD by mutation of arginine 279 to glutamic acid at the phosphate-binding cassette [17] ($EPAC1_{R279E}$-CFP) that gives no FRET signal between $EPAC1_{R279E}$-CFP and 8-Fluo-cAMP (Fig. S1). Therefore, our FRET-based assay detects the specific molecular interaction between the CNBD and the cAMP analogue. We observed the highest FRET efficiency (0.81 ± 0.05) upon mixing 50 nM CNBD-CFP with 500 nM 8-Fluo-cAMP. As an additional positive example of our method, we prepared CNBD-CFP using the CNBD of CAP/CRP, a transcription factor of prokaryote (CAP/CRP_{CNBD}-CFP) and observed specific FRET signal between CAP/CRP_{CNBD}-CFP and 8-Fluo-cAMP in micromolar range (Fig. S2).

Binding assay using unpurified proteins

In the next experiment, we performed the same binding assay using unpurified protein, namely the soluble extract of the bacteria that contains many endogenous proteins besides $EPAC1_{CNBD}$-CFP. Figure 3 shows that our method still allows us to detect the specific interaction between $EPAC1_{CNBD}$-CFP and 8-Fluo-cAMP. The FRET efficiency of the unpurified $EPAC1_{CNBD}$-CFP is slightly lower than that of the purified protein. This is probably due to the interference from endogenous proteins that interact with cAMP and partial degradation of $EPAC1_{CNBD}$-CFP.

Association and dissociation rate constants

It is possible to measure the kinetics of the molecular interaction between $EPAC1_{CNBD}$-CFP and 8-Fluo-

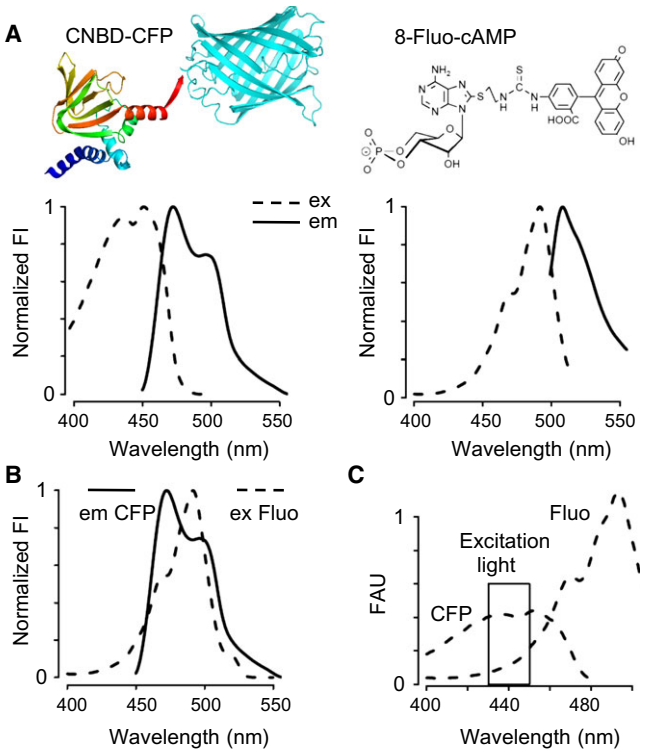

Fig. 1. Structure and fluorescence spectra of EPAC1$_{CNBD}$-CFP and 8-Fluo-cAMP. Panel A shows chemical structures (upper part) and fluorescence spectra (lower part) of EPAC1$_{CNBD}$-CFP and 8-Fluo-cAMP (left and right respectively). Since crystal structure of EPAC1 is not available, the corresponding 3D structure of EPAC2 was used to illustrate the structure of EPAC1$_{CNBD}$-CFP. Fluorescence spectra are shown as normalized fluorescence intensities (Normalized FI). Panel B shows the overlap between the CFP emission spectrum (em CFP) and 8-Fluo-cAMP excitation spectrum (ex Fluo). Panel C shows excitation spectra of EPAC1$_{CNBD}$-CFP (CFP) and 8-Fluo-cAMP (Fluo), whose fluorescence emissions were detected at 485 nm and 515 nm respectively. Fluorescence intensities are shown as fluorescence arbitrary units (FAU). In all panels, dashed lines represent the excitation spectrum and continuous lines represent the emission spectra. Each spectrum is representative of more than three measurements.

cAMP by monitoring the FRET signal in real time. Therefore, we determined the association and dissociation rate constants between EPAC1$_{CNBD}$-CFP and 8-Fluo-cAMP using stopped-flow spectrofluorometer. Figure 4A shows representative dissociation kinetics when excess of 8-CPT-cAMP (10 μM) was added to EPAC1$_{CNBD}$-CFP/8-Fluo-cAMP complex (100 nM of each compound). Figure 4B shows representative association kinetics of 100 nM EPAC1$_{CNBD}$-CFP and 100 nM 8-Fluo-cAMP. In both figures, black dots indicate the experimental data and red lines indicate best-fit curves using Eqn (2) as described in Materials and methods. We also performed the same binding kinetics measurements in the presence of 100 mM imidazole in order to determine the effect of this compound on the molecular interaction (Table 1). There is no statistical difference in the association rate constants (k_{on}) between the two conditions, but the dissociation rate constant (k_{off}) with imidazole is statistically smaller. However, there is no statistical difference in dynamic K_d (k_{off}/k_{on}) values between the two conditions (3.65 ± 0.07 nM and 3.64 ± 0.08 nM in the absence and presence of imidazole respectively). Therefore, we consider that the effect of residual imidazole (30 mM at highest and < 2 mM in most conditions in our experiments) on the molecular interaction between EPAC1$_{CNBD}$-CFP and 8-Fluo-cAMP would be negligible.

Dissociation constant obtained by fluorescence spectroscopy in equilibrium-binding condition

Dissociation constant (K_d) is usually determined by mixing a fixed amount (concentration) of a receptor with various concentrations of a ligand until the receptor saturation, then the free and bound ligand concentrations in each sample at equilibrium are measured to calculate the K_d value (free ligand concentration which allows 50% occupation of the receptor). Since both the ligand and the receptor are fluorescently labelled in our system with significant spectral overlap, it will be required to determine the net CFP fluorescence intensities by subtraction of background fluorescence

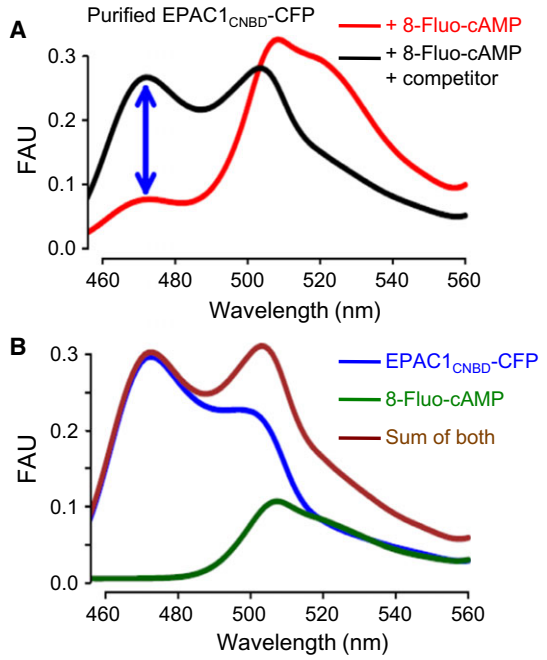

Fig. 2. Fluorescence spectra of $EPAC1_{CNBD}$-CFP and 8-Fluo-cAMP. Panel A shows the fluorescence spectra of 100 nM $EPAC1_{CNBD}$-CFP + 200 nM 8-Fluo-cAMP in the presence (black line) of absence (red line) of excess of competitor (10 μM 8-CPT-cAMP). Two-headed arrow indicates the occurrence of FRET in this condition. Panel B shows individual fluorescence spectra of 100 nM $EPAC1_{CNBD}$-CFP (blue line), 200 nM 8-Fluo-cAMP (green line) and the sum of the two spectra (brown line). Fluorescence intensities are shown as fluorescence arbitrary units (FAU). Representative spectra of more than three measurements are shown.

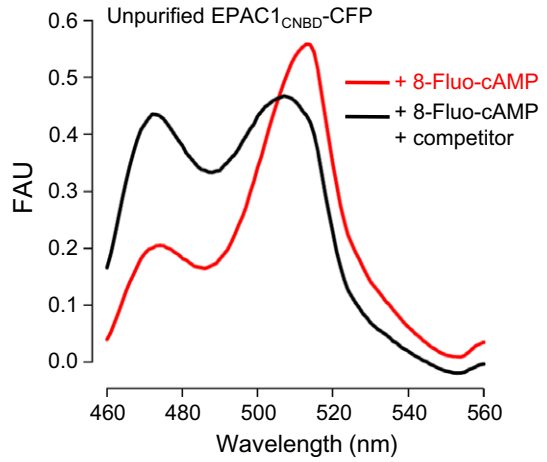

Fig. 3. Binding assay using unpurified $EPAC1_{CNBD}$-CFP. The emission fluorescence spectra of the unpurified $EPAC1_{CNBD}$-CFP (donor, 100 nM) + 8-Fluo-cAMP (acceptor, 200 nM) in the presence (black line) and absence (red line) of 8-CPT-cAMP (10 μM) are shown. Fluorescence intensities are shown as fluorescence arbitrary units (FAU). Representative spectra of more than three measurements are shown.

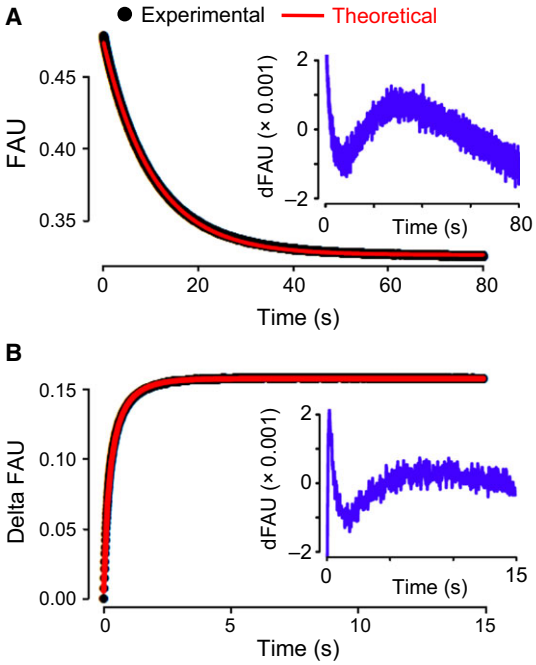

Fig. 4. Binding kinetics measurements by stopped-flow spectrofluorometry. Panel A shows the changes of fluorescence intensities (> 515 nm excited at 440 nm) measured by stopped-flow spectrofluorometry upon addition of 10 μM 8-CPT-cAMP to the mixture of 100 nM $EPAC1_{CNBD}$-CFP and 100 nM 8-Fluo-cAMP (back dots). Theoretical values (red line) were obtained by best fitted to single exponential decay. Fluorescence intensities are shown as fluorescence arbitrary units (FAU). Inset shows the difference (dFAU) between experimental results and the theoretical values. Panel B shows changes of the fluorescence intensities upon mixing 100 nM $EPAC1_{CNBD}$-CFP and 100 nM 8-Fluo-cAMP (back dots) and a best-fitted curve using Eqn (2) (red line). Fluorescence intensities are shown as the net change in fluorescence arbitrary units (Delta FAU) so that the initial value would be 0. Inset shows the difference (dFAU) between experimental results and the theoretical values. Representative traces of three measurements are shown.

intensities of the ligand (8-Fluo-cAMP fluorescence excited by 440 nm light) in all experimental conditions to calculate FRET efficiency. Particularly, when excess amounts of the ligand (8-Fluo-cAMP) against the receptor ($EPAC1_{CNBD}$-CFP) are used, this process (subtraction of background fluorescence intensities of the ligand, 8-Fluo-cAMP) will be indispensable. For further accurate experiments, we have to add an excess amount of competitor to all series of samples to obtain FRET value in each condition. To simplify this laborious process, we performed a binding experiment between $EPAC1_{CNBD}$-CFP and 8-Fluo-cAMP in a constant stoichiometry (1 : 2) in the absence and presence of an excess of competitor (8-CPT-cAMP). Then, various concentrations of the ligand and the receptor

Table 1. Rate constants of the molecular interaction between $EPAC1_{CNBD}$-CFP and 8-Fluo-cAMP.

	Without imidazole	With 100 mM imidazole
Number of measurements	5	5
k_{on} ($\times 10^7$ $M^{-1}{\cdot}s^{-1}$)	2.62 ± 0.05	2.59 ± 0.05
k_{off} ($\times 10^{-2}{\cdot}s^{-1}$)	9.55 ± 0.02	9.42 ± 0.02*
K_d (k_{off}/k_{on}) (nM)	3.65 ± 0.07	3.64 ± 0.08

*$P < 0.05$ Wilcoxon rank sum test.

were prepared merely by serial dilution as described in Materials and methods. The FRET efficiencies of each condition were calculated as the peak fluorescence intensity of the CFP (λ_{em} 474 nm) divided with that of the isosbestic point (λ_{em} 501 nm), which is determined by donor–acceptor stoichiometry but independent of sample concentrations as observed in Fig. S3. Figure 5 shows FRET efficiency between $EPAC1_{CNBD}$-CFP and 8-Fluo-cAMP plotted in the function of the total (not free) ligand concentration. The K_d value of each experiment was determined by best-fitting as described in materials and methods. We obtained a K_d value of 5.7 ± 2.6 nM ($n = 5$) in the equilibrium condition (static K_d), which is comparable to dynamic K_d value (3.65 ± 0.07 nM). In order to validate the static K_d value determined by FRET-based method, we also performed the similar binding experiments (equilibrium binding condition) by measuring the anisotropy of 8-Fluo-cAMP (Fig. S4). The K_d value obtained by anisotropy is 15.8 ± 3.5 nM ($n = 3$), which is slightly higher than, but comparable to, the value obtained by our FRET-based method. These K_d values of 8-Fluo-cAMP to CNBD of human EPAC1 are much lower than that of cAMP (4 μM) [4,5]. In other words, the affinity of this fluorescent analogue to the CNBD is much higher than intact cAMP.

Competition curve with cNMPs

In order to prove the versatility of our methods, we also performed competitive binding assay using cAMP, cGMP and their 8-CPT analogues as described in Materials and methods. As expected, cAMP has a higher competitive activity than cGMP (Fig. 6). Each 8-CPT-cNMP analogue has a higher activity than the intact cNMP as previously demonstrated [16], which indicates that addition of an alkyl group at carbon-8 of cyclic cNMP increases the affinity to the CNBD in general although a ligand with high affinity does not always serve as a potent EPAC activator [5,16,18]. We calculated the K_i values (K_d value of competitors) using Wang′s method [15] (with 5.7 nM as the K_d value of 8-Fluo-cAMP): 8-CPT-cAMP (250 nM), cAMP (3.8 μM), 8-CPT-cGMP (22 μM) and cGMP (140 μM). The K_i value of cAMP determined in this study is almost equal to the K_d values reported previously 4.0–4.2 μM (CNBD149–318)[4,5]. On the other hand, when the K_d value obtained by Anisotropy (15.8 nM) is used for the calculation, the K_i value of cAMP (7.0 μM) is slightly higher than the value previously reported. This result also supports the relevance of our FRET-based binding experiment. The K_i value of 8-CPT-cAMP (250 nM) is smaller than that of cAMP, however, it is still larger than the K_d of 8-Fluo-cAMP determined in this study.

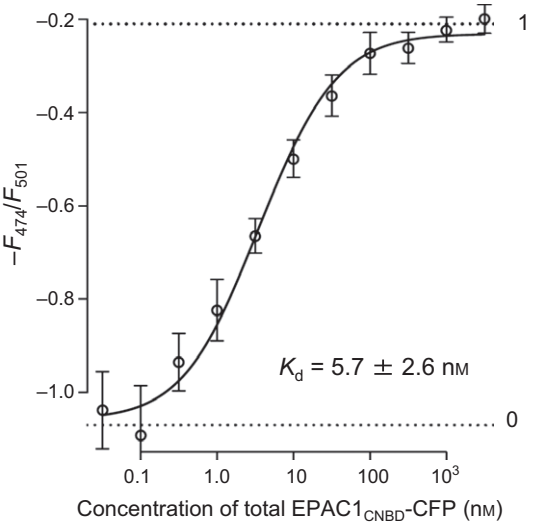

Fig. 5. Molecular affinity determination at equilibrium binding. Equilibrium-binding assays were performed using a fixed stoichiometry of $EPAC1_{CNBD}$-CFP and 8-Fluo-cAMP (1 : 2) in different concentrations as described in Materials and methods. Index of FRET efficiencies ($-F_{474}/F_{501}$, averages of three measurements ± SD) were plotted in function of the total concentration of $EPAC1_{CNBD}$-CFP (circles). The fraction of the $EPAC1_{CNBD}$-CFP bound to 8-Fluo-cAMP is indicated with dotted lines from 0 to 1. The K_d value was determined as described in Materials and methods. The best-fit curve using Eqn (4) is drawn with black line.

Discussion

In this work, we developed a simple FRET-based technique to study the molecular interactions between a recombinant CNBD and a fluorescent analogue of cNMP. In our methods, the recombinant CNBD is prepared as a fusion protein with fluorescent protein (FP). Therefore, in association with the property of FP, there are several advantages to perform experiments: (a) increased solubility of the recombinant protein, (b) visual tracking of the recombinant protein during the expression, extraction and purification, and (c) determination of the protein concentration using

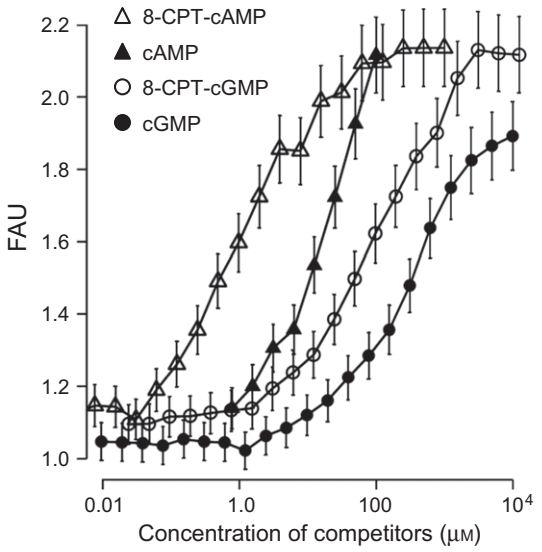

Fig. 6. Competitive binding curves determined by fluorescence plate reader. The fluorescence intensities of the CFP were determined by fluorescence plate reader from the mixture of 10 nM $EPAC1_{CNBD}$-CFP and 20 nM 8-Fluo-cAMP in the presence of four distinct competitors with distinct concentration prepared by serial dilution: 8-CPT-cAMP (open triangle), cAMP (closed triangle), 8-CPT-cGMP (open circle) and cGMP (closed circle). The averages of three measurements ± SD are shown. IC_{50} values of 8-CPT-cAMP, cAMP, 8-CPT-cGMP and cGMP are 1.1, 17, 98 and 600 μM respectively.

absorbance of FP. Considering all these features, our FRET-based binding assay is a user-friendly method to study molecular interaction between CNBD and cNMP.

Currently, there are two popular methods based on fluorescence spectroscopy – fluorescence anisotropy and fluorescence enhancement – to study molecular interaction between CNBD and cNMP. Fluorescence anisotropy is an elegant technique and provides reliable results in a binding experiment. However, it is not so versatile as FRET measurements because special equipment (mobile polarizers) is required to perform this experiment [19]. Moreover, the sensitivity of anisotropy determination is diminished as the consequence of reduction of fluorescence signals passed through polarizers. Indeed, we did not use the results of anisotropy obtained with less than the 10 nM of 8-Fluo-cAMP to calculate the K_d value since the deviation of anisotropy value of 3.16 and 1 nM of 8-Fluo-cAMP was quite large in our system owing to use of monochromator instead of bandpass filter to select emission light. In this sense, FRET-based binding assay is likely to be more sensitive than that of anisotropy. On the other hand, fluorescence enhancement using 8-NBD-cAMP can be performed with a conventional spectrofluorometer [6]. Nevertheless, NBD is not as bright as CFP. In our measurement, the fluorescence intensity of 8-NBD-cAMP in aqueous solution is ~ 900 times dimmer than that of CFP. In general, the fluorescence intensity of 8-NBD-cAMP increases several times upon binding to isolated CNBD [6,10], and this enhanced fluorescence intensity of NBD is much lower than that of CFP. As a particular case, it was reported that 8-NBD-cAMP showed a 100-fold increase in its fluorescence upon binding to EPAC2 [11]. However, this bright state of 8-NBD-cAMP is still dimmer than CFP. Therefore, the technique with 8-NBD-cAMP requires higher concentration of ligand and receptor (60–100 nM) [11] than our method (10–20 nM) for a reliable binding assay in convectional fluorescence plate reader. Therefore, our FRET-based technique is more versatile and sensitive than the assays based on fluorescence spectroscopy described above. Since a K_d value of any ligand–receptor interactions can be more accurately determined using the receptor concentration close to (or less than) its K_d value, the FRET-based method is a suitable technique to study high affinity (nM range) interactions.

Another prominent feature of our method is that it is possible to perform the binding assay with unpurified recombinant protein. This feature may allow us to study uncharacterized cNMP-binding proteins efficiently. A recent bioinformatic analysis revealed that there are many predicted CNBDs in uncharacterized proteins in both prokaryotes and eukaryotes [1,20]. At least, there are three well-defined examples, in which their putative CNBDs do not function as canonic CNBDs: prokaryote transcriptional factors CooA y CprK [21,22] and voltage-dependent K^+ channels (KCNH) [23,24]. Therefore, it is necessary to confirm the activity of those predicted CNBDs by experiments using natural or recombinant proteins. Our method should work for this purpose.

In spite of the usefulness of the assay, there are some disadvantages in our method. One of the negative properties is that the fluorescence spectra of CFP and fluorescein are too close each other and the excitation light for CFP slightly, but significantly, excites fluorescein (Figs 1C and 2B). This property makes us difficult to perform typical binding experiment to obtain static K_d value in the equilibrium condition. In order to overcome this problem, we performed an equilibrium-binding experiment with a constant stoichiometry of the ligand and the receptor but different absolute concentrations (Fig. 5). In our knowledge, this method had never been used before, but it can be an alternative method to determine a K_d value for

molecular interactions. The K_d value of 8-Fluo-cAMP determined in this study (5.7 nM) is much smaller than that of cAMP (4 μM) and even smaller than that of 8-CPT-cAMP (250 nM, K_i value determined in this study). The k_{on} of 8-Fluo-cAMP to the CNBD of EPAC1 determined in this study (2.6×10^7 $M^{-1} \cdot s^{-1}$) is closed to that of 8-MABA-cAMP reported previously (1.4×10^7 $M^{-1} \cdot s^{-1}$) [5]. On the other hand, the k_{off} of 8-Fluo-cAMP from the CNBD (0.096 s^{-1}) is more than 200 times smaller than that of 8-MABA-cAMP (22 s^{-1}). Therefore, the difference of K_d values between 8-Fluo-cAMP (5.7 nM in this study) and 8-MABA-cAMP (1.6 μM, previously obtained by ITC) can be principally attributed to the difference of their k_{off} values. Namely, the slow dissociation of 8-Fluo-cAMP from the CNBD can explain its high affinity to the CNBD.

Finally, we should keep in our mind that the study of molecular interactions using a partial protein such as an isolated CNBD does not fully reflect the activity of this domain under the physiological conditions. Therefore, the physiologically relevant parameters, such as K_d and ligand specificity, should be obtained using the entire protein instead of an isolated domain.

Conclusion

In this study, we developed a straightforward and reliable method to study molecular interaction between cNMP and CNBD based on intermolecular FRET. Currently, *in vivo* intermolecular FRET is a popular technique to study protein–protein interactions, in which each protein is tagged with a FP with a distinct fluorescence spectrum. In our case, we employed a small molecule tagged with a chemically synthesized fluorophore (fluorescein) as the FRET acceptor to study the interaction between a cyclic nucleotide and its binding protein, CNBD, tagged with CFP as the FRET donor. This would be a useful method to study poorly characterized or predicted CNBDs. Considering the technical advantages of our method, the same principle can also be applied to many other binding assays such as ligand–receptor and antigen–antibody interactions.

Acknowledgements

We thank Dr. Takeharu Nagai (Osaka University) and Dr. Martin Lohse (Wuerzburg University) for providing mseCFP-pRSETB and EPAC1-camps-pcDNA respectively. We appreciate National Institute of Genetics for providing two *E. coli* strains, JM109 (DE3) and BL21 (DE3). We thank Eugenio López, Santiago Becerra, Jorge Yáñez and Paul Gaytán for oligonucleotides and DNA synthesis and plasmid sequencing.

Author contribution

TN designed the whole project. FR carried out stopped-flow fluorometry, fluorescence spectroscopy of equilibrium binding, competitive assays, anisotropy measurements and mutagenesis of EPAC1. CSC designed oligonucleotides for mutagenesis. CSC and YSG prepared the CNBD-CFP plasmid and performed the initial FRET measurements. TN and FR wrote the manuscript, but all authors were involved in the manuscript preparation.

Funding

This work was supported by PAPIIT DGAPA-UNAM (IN206116 and IN203513 to TN) and by CONACyT (128566 and 177138 to TN). FR, CSC and YSG are graduate students supported by CONACyT.

References

1 Kannan N, Wu J, Anand GS, Yooseph S, Neuwald AF, Venter JC and Taylor SS (2007) Evolution of allostery in the cyclic nucleotide binding module. *Genome Biol* **8**, R264.

2 Krähling AM, Alvarez L, Debowski K, Van Q, Gunkel M, Irsen S, Al-Amoudi A, Strünker T, Kremmer E, Krause E *et al.* (2013) CRIS-a novel cAMP-binding protein controlling spermiogenesis and the development of flagellar bending. *PLoS Genet* **9**, e1003960.

3 Saraswat LD, Ringheim GE, Bubis J and Taylor SS (1988) Deletion mutants as probes for localizing regions of subunit interaction in cAMP-dependent protein kinase. *J Biol Chem* **263**, 18241–18246.

4 de Rooji J, Rehmann H, van Triest M, Cool RH, Wittinghofer A and Bos JL (2000) Mechanism of regulation of the Epac family of cAMP-dependent RapGEFs. *J Biol Chem* **275**, 20829–20836.

5 Kraemer A, Rehmann HR, Cool RH, Theiss C, de Rooij J, Bos JL and Wittinghofer A (2001) Dynamic interaction of cAMP with the Rap guanine-nucleotide exchange factor Epac1. *J Mol Biol* **306**, 1167–1177.

6 Cukkemane A, Gruter B, Novak K, Gensch T, Bonigk W, Gerharz T, Kaupp UB and Seifert R (2007) Subunits act independently in a cyclic nucleotide-activated K(+) channel. *EMBO Rep* **8**, 749–755.

7 Khwaja TA, Boswell KH, Robins RK and Miller JP (1975) 8-Substituted derivatives of adenosine 3′,5′-cyclic phosphate require an unsubstituted 2′-hydroxyl group in the ribo configuration for biological activity. *Biochemistry* **14**, 4238–4244.

8 Moll D, Prinz A, Brendel CM, Berrera M, Guske K, Zaccolo M, Genieser HG and Herberg FW (2008) Biochemical characterization and cellular imaging of a novel, membrane permeable fluorescent cAMP analog. *BMC Biochem* **9**, 18.
9 Scott SP, Shea PW and Dryer SE (2007) Mapping ligand interactions with the hyperpolarization activated cyclic nucleotide modulated (HCN) ion channel binding domain using a soluble construct. *Biochemistry* **46**, 9417–9431.
10 Brelidze TI, Carlson AE and Zagotta WN (2009) Absence of direct cyclic nucleotide modulation of mEAG1 and hERG1 channels revealed with fluorescence and electrophysiological methods. *J Biol Chem* **284**, 27989–27997.
11 Tsalkova T, Mei FC and Cheng X (2012) A fluorescence-based high-throughput assay for the discovery of exchange protein directly activated by cyclic AMP (EPAC) antagonists. *PLoS ONE* **7**, e30441.
12 Nikolaev VO, Bunemann M, Hein L, Hannawacker A and Lohse MJ (2004) Novel single chain cAMP sensors for receptor-induced signal propagation. *J Biol Chem* **279**, 37215–37218.
13 Heim R, Prasher DC and Tsien RY (1994) Wavelength mutations and posttranslational autoxidation of green fluorescent protein. *Proc Natl Acad Sci USA* **91**, 12501–12504.
14 R Core Team (2016) R: A Language and Environment for Statistical Computing. R Foundation for Statistical Computing, Vienna, Austria.
15 Nikolovska-Coleska Z, Wang R, Fang X, Pan H, Tomita Y, Li P, Roller PP, Krajewski K, Saito NG, Stuckey JA *et al*. (2004) Development and optimization of a binding assay for the XIAP BIR3 domain using fluorescence polarization. *Anal Biochem* **332**, 261–273.
16 Rehmann H, Schwede F, Doskeland SO, Wittinghofer A and Bos JL (2003) Ligand-mediated activation of the cAMP-reponsive guanine nucleotde exchange factor EPAC. *J Biol Chem* **278**, 38548–38556.
17 Qiao J, Mei FC, Popov VL, Vergara LA and Cheng X (2002) Cell cycle-dependent subcellular localization of exchange factor directly activated by cAMP. *J Biol Chem* **277**, 26581–26586.
18 Schwede F, Bertinetti D, Langerijs CN, Hadders MA, Wienk H, Ellenbroek JH, de Koning EJ, Bos JL, Herberg FW, Genieser HG *et al*. (2015) Structure-guided design of selective Epac1 and Epac2 agonists. *PLoS Biol* **13**, e1002038.
19 Lakowicz JR (2006) Principles of Fluorescence Spectroscopy, 3rd edn. Springer, University of Maryland School of Medicine, Baltimore, MD.
20 Mohanty S, Kennedy EJ, Herberg FW, Hui R, Taylor SS, Langsley G and Kannan N (2015) Structural and evolutionary divergence of cyclic nucleotide binding domains in eukaryotic pathogens: implications for drug design. *Biochim Biophys Acta* **1854**, 1575–1585.
21 Lanzilotta WN, Schuller DJ, Thorsteinsson MV, Kerby RL, Roberts GP and Poulos TL (2000) Structure of the CO sensing transcription activator CooA. *Nat Struct Biol* **7**, 876–880.
22 Joyce MG, Levy C, Gábor K, Pop SM, Biehl BD, Doukov TI, Ryter JM, Mazon H, Smidt H, van den Heuvel RH *et al*. (2006) CprK crystal structures reveal mechanism for transcriptional control of halorespiration. *J Biol Chem* **281**, 28318–28325.
23 Brelidze TI, Carlson AE, Sankaran B and Zagotta WN (2012) Structure of the carboxy-terminal region of a KCNH channel. *Nature* **481**, 530–533.
24 Marques-Carvalho MJ, Sahoo N, Muskett FW, Vieira-Pires RS, Gabant G, Cadene M, Schonherr R and Morais-Cabral JH (2012) Structural, biochemical, and functional characterization of the cyclic nucleotide binding homology domain from the mouse EAG1 potassium channel. *J Mol Biol* **423**, 34–46.

Supporting information

Additional Supporting Information may be found online in the supporting information tab for this article:
Fig. S1. Fluorescence spectra of $CNBD_{R279E}$-CFP and 8-Fluo-cAMP.
Fig. S2. Fluorescence spectra of CAP/CRP_{CNBD}-CFP and 8-Fluo-cAMP.
Fig. S3. Fluorescence spectra of the mixture of $EPAC1_{CNBD}$-CFP and 8-Fluo-cAMP (1:2 stoichiometry) in the absence (red line) or the presence (black line) of the competitor (8-CPT-cAMP).
Fig. S4. Fluorescence anisotropy of 8-Fluo-cAMP at equilibrium binding.